

DESIGN AND ANALYSIS OF A HIGH POWER 1 KHZ MAGNETIC MODULATOR

Howard Rhinehart and Roger Dougal
University of South Carolina
Electrical Engineering Department
Columbia, SC 29208

W.C. Nunnally
Los Alamos National Laboratory
Electronics Division
Los Alamos, NM 87545

Abstract

This paper describes a magnetic modulator which was designed for second generation use in the Proton Storage Ring at the Los Alamos Meson Physics Facility. The three stage machine delivered a 25 kV, 100 nanosecond pulse to a 3 ohm load at pulse repetition rates of up to 1 kHz. A principle function of this system was to serve as a test bed for the measurement of energy losses in magnetic switches. The magnetic switch cores were built from materials of two different alloys, and were tested in both as-cast and annealed states. The performance data acquired indicate that annealing of the core material reduces energy loss by up to a factor of five and that, as expected, losses are lower in the higher resistivity materials.

Modulator Design

A three stage magnetic pulse compression system[1] has been designed to prove the feasibility of using magnetic switching techniques to supply the pulsed excitation for an extraction system at the Los Alamos Meson Physics Facility's Proton Storage Ring (PSR). Pulse parameter requirements for the PSR are presented in Table 1.

Table 1

Proton Storage Ring Pulse Parameters

Voltage	40 kV
Duration	50 ns
Load Impedance	4 ohm
Peak Current	10 kA
Pulse Repetition Rate	1 kHz

The circuit diagram of the modulator which has been designed to meet these requirements is shown in Figure 1. The primary switch used in this modulator was a hydrogen thyratron, EG&G model 3024. The low voltage section of the modulator was resonantly charged from a 0-5 kV supply through a voltage doubler circuit. The primary capacitance was matched to the capacitance of the high voltage side of the modulator as referred through the 10:1 transformer. The inductor in the resonant charging circuit was selected to give a charging time of slightly less than 1 millisecond, thus allowing operation at up to 1 kHz.

This modulator is of the series magnetic circuit design[2], therefore each magnetic stage operates at the same design voltage of 80 kV. Power gain is obtained by decreasing the energy transfer time from stage to stage. Switching of the energy from one stage to the next is effected by the saturable inductors placed between the capacitive sections. As energy transfer efficiency is maximized by utilizing equal capacitances in each stage[2], we have chosen that design for this modulator. With equal capacitances in each stage, the resonant transfer time is determined by the value of inductance linking one stage with the next. This was varied, in turn, by the the number of conductor turns around the core. The pulse compression sequence was initiated by introduction of a 10 microsecond, 8 kV pulse to a 10:1 step-up transformer which delivered the energy to the first stage of the magnetic pulse compressor. This was compressed to a 2 microsecond pulse as the energy was delivered to the second stage, and further compressed to 400 nanoseconds as it was delivered to the third stage. Finally a 100 nanosecond duration pulse was delivered to the load at the output of the third stage. The last

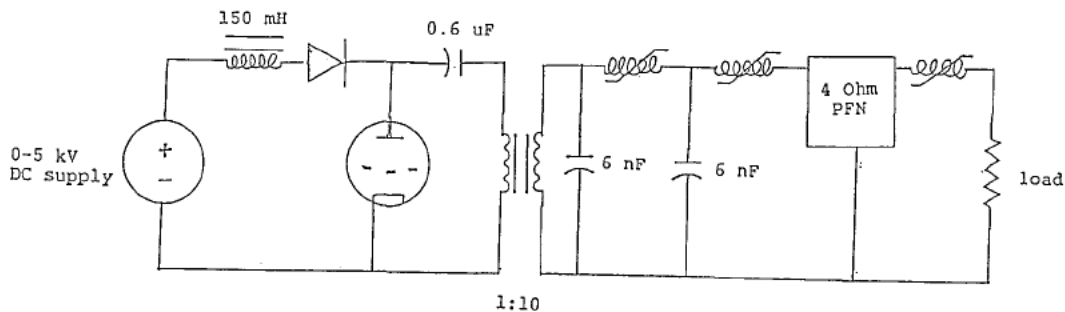


Figure 1. Modulator circuit diagram.

Report Documentation Page				Form Approved OMB No. 0704-0188	
Public reporting burden for the collection of information is estimated to average 1 hour per response, including the time for reviewing instructions, searching existing data sources, gathering and maintaining the data needed, and completing and reviewing the collection of information. Send comments regarding this burden estimate or any other aspect of this collection of information, including suggestions for reducing this burden, to Washington Headquarters Services, Directorate for Information Operations and Reports, 1215 Jefferson Davis Highway, Suite 1204, Arlington VA 22202-4302. Respondents should be aware that notwithstanding any other provision of law, no person shall be subject to a penalty for failing to comply with a collection of information if it does not display a currently valid OMB control number.					
1. REPORT DATE JUN 1985		2. REPORT TYPE N/A		3. DATES COVERED -	
4. TITLE AND SUBTITLE Design And Analysis Of A High Power 1 Khz Magnetic Modulator				5a. CONTRACT NUMBER	
				5b. GRANT NUMBER	
				5c. PROGRAM ELEMENT NUMBER	
6. AUTHOR(S)				5d. PROJECT NUMBER	
				5e. TASK NUMBER	
				5f. WORK UNIT NUMBER	
7. PERFORMING ORGANIZATION NAME(S) AND ADDRESS(ES) University of South Carolina Electrical Engineering Department Columbia, SC 29208				8. PERFORMING ORGANIZATION REPORT NUMBER	
9. SPONSORING/MONITORING AGENCY NAME(S) AND ADDRESS(ES)				10. SPONSOR/MONITOR'S ACRONYM(S)	
				11. SPONSOR/MONITOR'S REPORT NUMBER(S)	
12. DISTRIBUTION/AVAILABILITY STATEMENT Approved for public release, distribution unlimited					
13. SUPPLEMENTARY NOTES See also ADM002371. 2013 IEEE Pulsed Power Conference, Digest of Technical Papers 1976-2013, and Abstracts of the 2013 IEEE International Conference on Plasma Science. Held in San Francisco, CA on 16-21 June 2013. U.S. Government or Federal Purpose Rights License.					
14. ABSTRACT This paper describes a magnetic modulator which was designed for second generation use in the Proton Storage Ring at the Los Alamos Meson Physics Facility. The three stage machine delivered a 25 kV, 100 nanosecond pulse to a 3 ohm load at a repetition rates of up to 1 kHz. A principle function of this system was to serve as a test bed for the measurement of energy losses in magnetic switches. The magnetic switch cores were built from materials of two different alloys, and were tested in both as-cast and annealed states. The performance data acquired indicate that annealing of the core material reduces energy loss by up to a factor of five and that, as expected, losses are lower in the higher resistivity materials.					
15. SUBJECT TERMS					
16. SECURITY CLASSIFICATION OF:			17. LIMITATION OF ABSTRACT SAR	18. NUMBER OF PAGES 4	19a. NAME OF RESPONSIBLE PERSON
a REPORT unclassified	b ABSTRACT unclassified	c THIS PAGE unclassified			

stage of the network has an output impedance of 4 ohms to match the modulator impedance to the load impedance.

Two different magnetic materials were used for the switch cores, Allied's Metglas 2605 SC and 2605 CO. The former is iron based, the latter contains some cobalt. Both are amorphous alloys, manufactured by cooling molten material rapidly so as to prevent the formation of long range crystalline order. Although the differences between the two materials are slight, 2605 CO does have both a slightly higher resistivity and a higher saturation flux density. The switch cores were toroidal in shape, and were wound from the amorphous metal ribbon with insulating material between layers. Polysulfone was used as the insulating material for the as-cast cores and DuPont Kapton for the annealed cores as it could withstand the high temperatures involved in the annealing process. The actual annealing was performed by Allied. All cores used in the modulator were of the same size, for maximum efficiency[3].

Modulator Performance Data

All portions of the magnetic modulator were instrumented so that measurements of every inductor current and capacitor voltage could be made. Data acquisition was via a computerized system which employed a Tektronix 7612 digitizer. One of the unique features of this modulator was the provision for operation at a variable pulse repetition rate (PRR). This feature enabled data to be taken at three different frequencies -- 10 Hz, 100 Hz, and 1 kHz, to determine if the PRR had any affect on the operating parameters. Although the output pulse duration was somewhat longer than that specified for the PSR no extensive effort was expended in optimizing the modulator operating parameters to fit those requirements. Instead, since a primary purpose of this modulator was to provide a test bed for magnetic switching materials, the time was spent concentrating on evaluation of the magnetic processes.

Typical waveforms of the voltages across the thyatron and intermediate storage capacitors are shown in Figure 2. Figure 3 shows current waveforms from all three saturable inductors. The decreasing energy transfer times, indicating higher power levels as the pulse progresses toward the load, are evident in these figures. The output voltage pulse to the load is also shown in Figure 3.

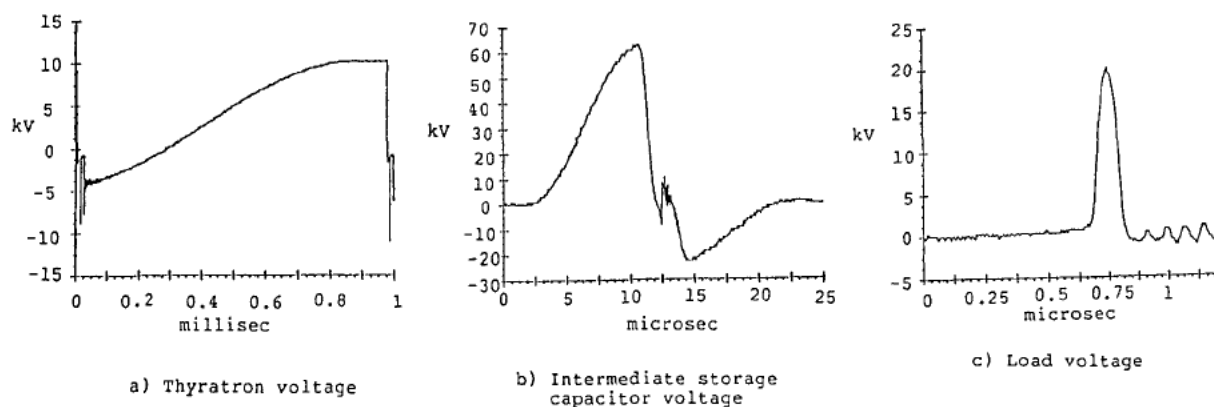


Figure 2. Circuit voltages.

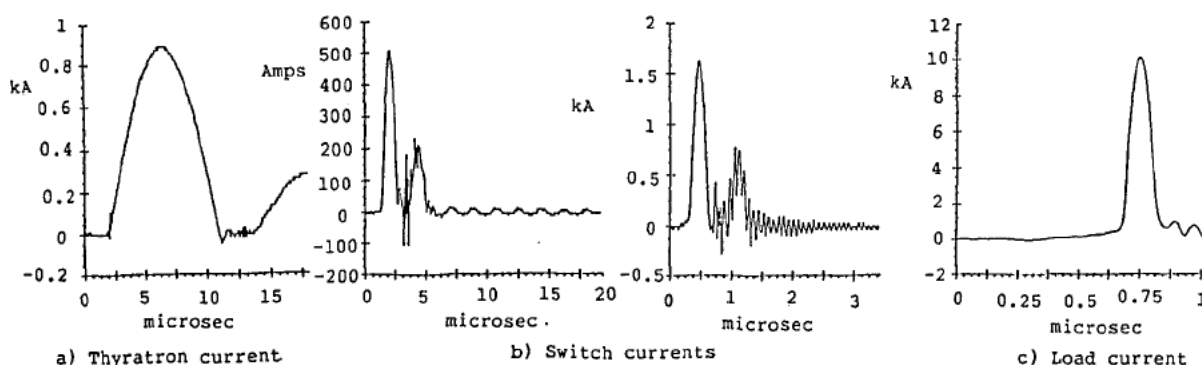


Figure 3. Circuit currents.

Several observations can be drawn directly from these data prior to any computational analysis; the stage-to-stage matching, as well as the matching of the PFN to the load, was not perfect, thus giving rise to some partial reflections of energy. Furthermore, the load impedance (as determined from load voltage and current) was not as expected. This can be attributed to the copper sulfate load resistor, which was somewhat difficult to adjust to the desired resistance value. As was stated previously, no attempt was made to optimize the performance.

Energy Losses

Switching energy losses were determined by numerically integrating the product of the switch back voltage and switch current from $t=0$ until the switch core saturated. In order to properly carry out this computation, the back voltage and current had to be properly aligned temporally. Due to the manner in which the data acquisition system was operated, this relationship was lost in taking the raw data. Computer

post-processing of the data restored the time reference and also corrected the back voltage for stray (non-magnetic) inductance. Filtering of post-saturation noise contributed by stray inductances and capacitances was also performed at this time. The results of this process are illustrated in Figure 4, in which the magnitudes of the displayed waveforms have been normalized in order to display both voltage and current on the same graph. The total flux swing and core B-H relationship were also obtained from the switch back voltage and current waveforms. Typical curves are shown in Figure 5 along with a typical curve of the total energy loss.

One of the major objectives of this experiment was to determine the effects of saturation time and annealing state on the overall energy losses. Total energy loss curves as a function of saturation time are shown in Figure 6 for both as-cast and annealed materials. These curves show that losses increase drastically as saturation time decreases. Also clearly seen in these curves is the effect of annealing on losses,

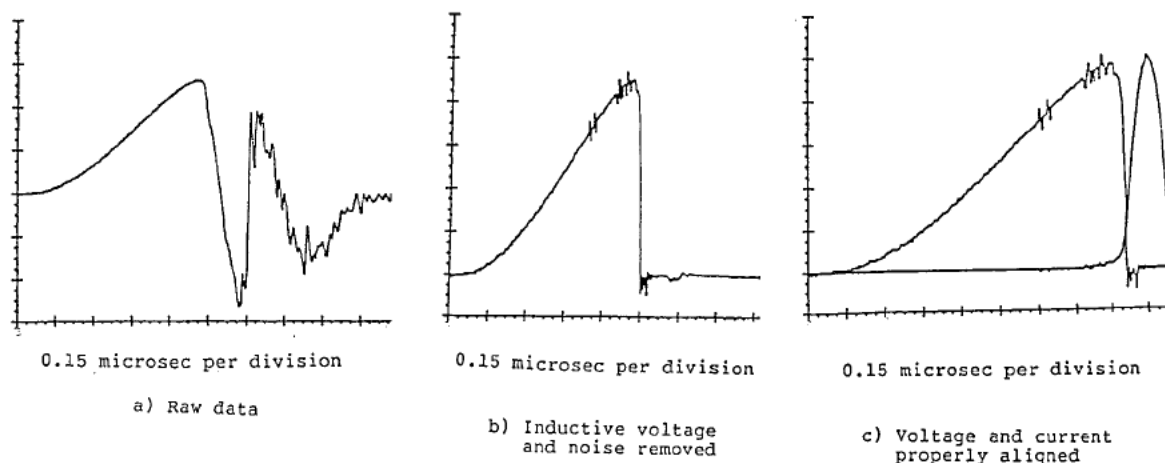


Figure 4. Data post-processing for energy losses.

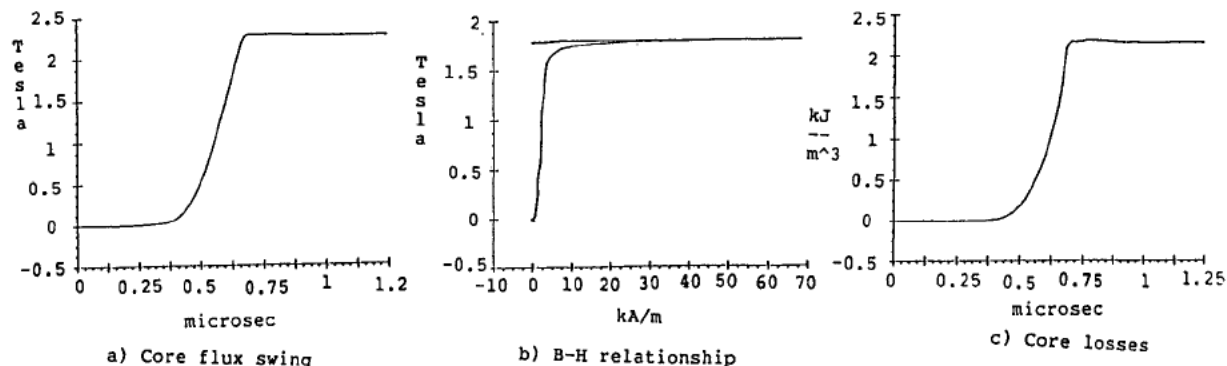


Figure 5. Data calculated from switch current & back voltage.

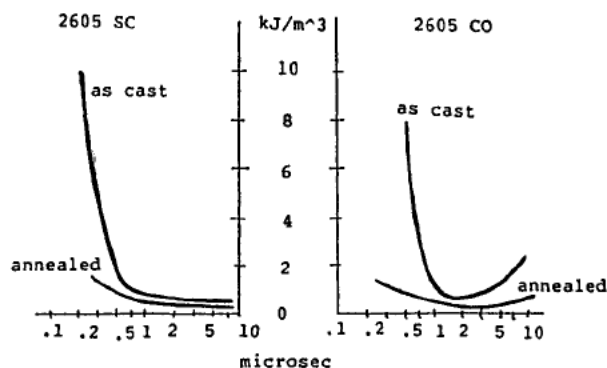


Figure 6. Energy losses vs saturation time.

especially in the faster region. The as-cast material exhibited total losses of up to 10 kJ/m^3 , whereas losses were reduced to under 2 kJ/m^3 by annealing. The data were essentially the same for all three pulse repetition rates.

There appeared to be some anomalies in the energy loss data acquired for the type 2605 CO material, so some of the cores were disassembled in an attempt to find a physical justification for those unexpected results. In at least two cases it was discovered that a part of the core had been shorted by the protective aluminum corebox in which the cores were mounted. This had the effect of greatly increasing the eddy current losses, and thus offsetting the decrease in eddy current losses which was expected to be found for the 2605 CO material due to its higher resistivity[4] (as compared to the 2605 SC material). (Resistivity of 2605 CO = 130 microhm-cm, resistivity of 2605 SC = 125 microhm-cm.) In fact, the as-cast 2605 CO material did perform better than the as-cast 2605 SC in the fastest section of the modulator, with total losses of only 8 kJ/m^3 versus almost 10 kJ/m^3 for the 2605 SC.

Conclusions

Magnetic energy losses in saturable inductor cores have been evaluated at three different pulse repetition rates for both as-cast and annealed cores of two different amorphous magnetic alloys. Total energy losses were reduced by up to a factor of five by use of annealed material rather than the as-cast material. No significant differences in energy losses were observed as pulse repetition rate was varied from 10 Hz to 1 kHz.

Two different amorphous alloys were used -- Metglas 2605 SC (an iron based alloy) and Metglas 2605 CO (which contains cobalt). Unfortunately meaningful comparisons between the two alloys cannot easily be drawn due to the evidence of arcing in the 2605 CO coreboxes. In spite of these faults in the core construction, the 2605 CO alloy did have slightly lower total losses than the 2605 SC for fast saturation times.

Analysis of the data is continuing. A computer simulation of the experiment is being prepared to calculate theoretical energy losses and to partition those losses amongst the various known loss mechanisms. Comparison of the measured losses with the calculated losses will divulge the anomalous loss component which, if large, may invite future investigation into its source.

References

1. W.S. Melville, "The Use of Saturable Reactors as Discharge Devices for Pulse Generators," Proc. Inst. Electr. Engr. (IEE, London, 1951) Vol. 98, Pt. 3, pp. 185-207.
2. W.C. Nunnally, "Magnetic Switches and Circuits," Los Alamos National Laboratory publication LA-8862-MS
3. R.A. Mathias and E.M. Williams, "Economic Design of Saturating Reactor Magnetic Pulsers," Trans. Amer. Inst. Electr. Eng. in Communications and Electronics (AIEE, New York, 1955), Vol. 74, No. 18, pp. 169-179.
4. C.H. Smith, "Metallic Glasses for Magnetic Switches," Fifteenth Power Modulator Symposium, Baltimore, Maryland, June 1982, pp. 22-27.